

# Production of defects in hexagonal boron nitride monolayer under ion irradiation

O. Lehtinen<sup>a,\*</sup>, E. Dumur<sup>a</sup>, J. Kotakoski<sup>a</sup>, A.V. Krasheninnikov<sup>a,b</sup>, K. Nordlund<sup>a</sup>, J. Keinonen<sup>a</sup>

<sup>a</sup> Department of Physics, University of Helsinki, P.O. Box 43, FI-00014 Helsinki, Finland

<sup>b</sup> Department of Applied Physics, Aalto University, P.O. Box 1100, FI-00076 Aalto, Finland

## ARTICLE INFO

### Article history:

Received 24 September 2010

Received in revised form 4 November 2010

Available online 18 November 2010

### Keywords:

Hexagonal boron nitride monolayer

Ion irradiation

Defect

## ABSTRACT

Atomistic computer simulations based on analytical potentials are employed to investigate the response of a hexagonal boron nitride monolayer to irradiation with noble gas ions having energies from 35 eV up to 10 MeV. Probabilities for creating different types of defects are calculated as functions of ion energy and incidence angle, along with sputtering yields of boron and nitrogen atoms. The presented results can be used for the optimization of ion processing of single-layer and bulk hexagonal boron nitride samples and for predicting the evolution of the material in radiation hostile environments.

© 2010 Elsevier B.V. All rights reserved.

## 1. Introduction

Hexagonal boron nitride (*h*-BN) monolayer [1,2] has a honeycomb structure similar to graphene [3], but alternating boron and nitrogen atoms substitute for carbon. While carbon atoms are covalently bonded in graphene, boron and nitrogen form ionic bonds in *h*-BN, so that this material possesses a gap of about 6 eV [4]. Similar to other wide gap semiconductors, the electronic and magnetic properties of this material may be governed by defects present in the lattice [5]. Moreover, if defects could be introduced in *h*-BN in a controllable manner, the properties of this material could be tailored, similar to carbon nanomaterials [6–9], facilitating the development of *h*-BN based devices.

One of the ways of introducing defects in *h*-BN is to expose it to energetic ion bombardment. Thus, the precise microscopic knowledge on the types and abundance of defects which appear under irradiation is required. It has been demonstrated however, that the traditional methods for estimating ion irradiation damage like the TRIM approach [10] fail in targets of low dimensionality [11] as detailed account of scattering processes at the atomic level is necessary for correct predictions of the response of nanoscale materials to ion irradiation. Although production of defects in BN nanomaterials under electron irradiation [12–17] and defect characteristics [18–21] have been studied at length, the atomic scale understanding of ion irradiation effects in this material is still lacking.

In this article, molecular dynamics simulations are employed to gain quantitative information on the probabilities for creating different types of defects in *h*-BN single layers under ion irradiation within a wide range of ion energies, ion species and angles of inci-

dence. This data can be used to select suitable irradiation parameters when aiming to introduce specific types of defects in a *h*-BN target for tailoring their properties with energetic particles, similar to other nano-materials [22,23]. Also, the evolution of *h*-BN in radiation hostile environment such as open space can be better understood based on the presented data.

## 2. Computational methods

Our molecular dynamics simulations (MD) were conducted using analytical potentials (AP) to investigate the effects of energetic noble gas ion impacts on a hexagonal boron nitride monolayer (*h*-BN). In our AP MD simulations the interactions between the boron and nitrogen atoms (B–N, B–B, N–N) were described by the Albe–Möller many-body potential [24,25], which is an analytical Tersoff-type potential fitted to a wide range of ab initio data. The potential reproduces well the formation energies of point defects in both *h*-BN and cubic boron nitride as compared to ab initio results. The potential describes the structure and energy of BN polymorphs and clusters as well as pure nitrogen and boron bonding. It has been previously used in simulations of bulk *h*-BN and BN nanotubes, including ion irradiation studies [26–28] where good agreement with the experimental data has been observed.

The interaction between the energetic noble gas (NG) ion (He, Ne, Ar, Kr and Xe) and the target boron and nitrogen atoms (NG–B/N) was described using the Ziegler–Biersack–Littmark universal repulsive potential [29]. Throughout this article we use term “ion” for direct analogy with the experiments, although the charge of the incoming atom is not explicitly considered, as this is beyond the AP MD approach. Besides this, the effects of low charge states are negligible. The AP MD method is computationally efficient enough for collecting a data set with statistically meaningful results

\* Corresponding author. Tel.: +358 9 191 50617; fax: +358 9 191 50610.

E-mail address: [ossi.lehtinen@helsinki.fi](mailto:ossi.lehtinen@helsinki.fi) (O. Lehtinen).

for the complicated parameter space of this study. Overall, our simulation setup is similar to what was used in Ref. [11] for graphene irradiation simulations.

The effects of electronic stopping on defect production was not taken into account in our simulations. Although loss of kinetic energy of the ion through inelastic collisions with target electrons is generally the dominant energy loss mechanism at high ion energies, it has been demonstrated that even at electronic stopping values of 17 keV/nm no structural modifications are introduced to *h*-BN [30,31]. Electronic stopping for all the ion–energy combinations considered in this article are well below this value, with a maximum value of 4 keV/nm for 10 MeV Xe and average value more than an order of magnitude less at all energies considered. Nevertheless, one can expect that the actual number of defects should be somewhat higher than predicted by our simulations, as a combination of ion–ion collisions and electronic excitations may give rise to additional defects [32].

A schematic illustration of the simulation setup is presented in Fig. 1. The target system, consisting of 400 B and 400 N atoms, is shown in Fig. 1(a). The impact points for ion irradiation were randomly selected within the minimum irreducible area of the lattice, Fig. 1(b) near the center of the system. Dissipation of heat waves created by the ion impact was simulated using the Berendsen thermostat [33] at the system edges with  $\Delta\tau = 10$  fs and target temperature 0 K. Adaptive time step, implemented in the simulation code PARCAS [34], was used in the simulations. Within this approach, the time step is determined based on the fastest moving particles in the system, resulting in timesteps ranging from attosecond scale to nearly one femtosecond. One picosecond after the ion impact, the resulting structure had typically reached a local energy minimum. Because the simulation times are too short for the structure to find the most stable local configuration, we heated the system for another picosecond, following the stimulated annealing approach we used in other simulations [35–37]. This facilitates further relaxation to allow removing at least the metastable structures with high potential energy. However, this annealing step did not significantly alter the results.

One set of simulations was carried out with all the incoming ions coming in with trajectory perpendicular to the sheet ( $\sim 150,000$  runs). Another set of simulations for examining the role of the angle of incidence was conducted varying the in-plane angle  $\varphi \in [0^\circ, 360^\circ]$  (Fig. 1b) and out-of-plane angle  $\theta \in [0^\circ, 88^\circ]$  (Fig. 1c). The angles  $\varphi$ ,  $\theta$  and impact points were chosen randomly and independently of each other. A total of  $\sim 1,000,000$  simulations were run to gather adequate statistics.

In order to check our model, we calculated the displacement threshold energies for boron ( $T_d^B$ ) and nitrogen ( $T_d^N$ ) and compared them to the results obtained by first-principles simulations.  $T_d$  can be defined as the minimum kinetic energy that must be delivered to an atom due to the impact of an energetic particle, in order for

the atom to leave its position in the atomic network and either take a metastable interstitial position in the lattice or leave the system. The following displacement thresholds were obtained:  $T_{d,APMD}^B = 17.98$  eV and  $T_{d,APMD}^N = 21.49$  eV, which are close to the results obtained by density-functional-theory MD:  $T_{d,DFT}^B = 19.36$  eV and  $T_{d,DFT}^N = 23.06$  eV [16]. The data are in a very good agreement taking into account the different level of sophistication of these two methods. Because the displacement threshold is the most important factor governing defect production under irradiation, and the utilized BN potential reproduces well the defect energetics [24], one can expect that the AP MD approach gives not only a qualitatively but also quantitatively good description of the simulated processes.

### 3. Results and discussion

#### 3.1. Ion trajectory perpendicular to the *h*-BN sheet

Having carried out AP MD simulations with sufficient statistics, we started the analysis of the results by calculating the average sputtering yield of B atoms, the average sputtering yield of N atoms and the sum of these two for all the ions as a function of ion energy, Fig. 2(a,b and c). Similarly to the case of graphene [11], sputtering yields first increase with energy until a peak value is reached, after which the yields decrease with increasing energy. This behavior can be explained by binary collision kinetics resulting in the drop of the cross-section for defect production at high energies [38]. Due to conservation of energy and momentum, a low energy ion needs to hit a target atom almost head-on for sufficient momentum transfer to occur. With increasing ion energy ion trajectories further from the target atom lead to ejection (corresponding to  $T > T_d^B$  or  $T > T_d^N$ ). After the peak value is reached the high velocity of the ion starts to decrease the sputtering probability as the duration of the ion–target atom interaction diminishes, leading to a requirement of a very close by trajectory of the ion to a target atom for the force of interaction to be strong enough to facilitate target atom sputtering.

To facilitate the analysis of the simulation data and to obtain a deeper understanding of defect production under ion irradiation, the defect structures produced by ion impacts were divided into four categories (single vacancies, double vacancies, complex vacancies and local amorphous areas), as described below. With low energies single vacancies (SV, exactly one atom missing from otherwise intact system) dominate as in carbon nanomaterials [39], Fig. 2(e, f and g), as the ion can barely displace one atom. With increasing ion energy ( $K_{ion} = 0.1 \dots 10$  keV), the ion can directly displace two target atoms creating double vacancies (DV, two atoms missing from otherwise intact system) at the expense of SVs. As ion energy gets even higher, the high velocity ion cannot pass close enough to more than one atom to displace it and

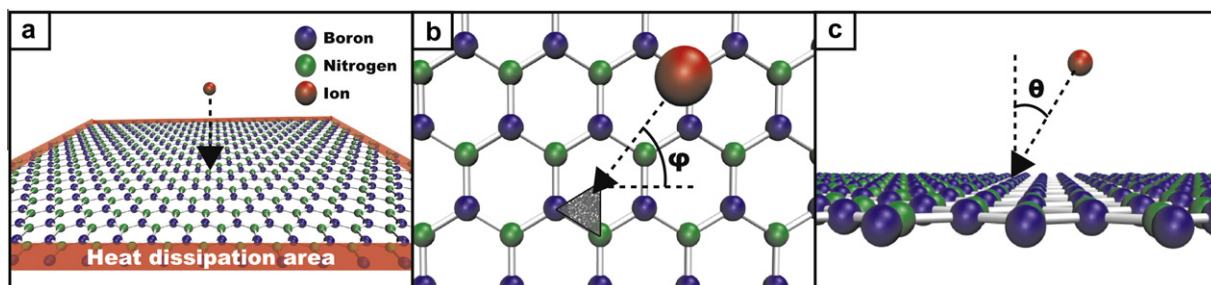


**Fig. 1.** A schematic illustration of the simulation setup. (a) The complete *h*-BN system with the heat dissipation area marked in red. (b) Definition of the in-plane-angle  $\varphi$  and a distribution of the points of ion impact (the grey triangle). (c) Definition of the out-of-plane angle  $\theta$ . (For interpretation of the references to colour in this figure legend, the reader is referred to the web version of this article.)

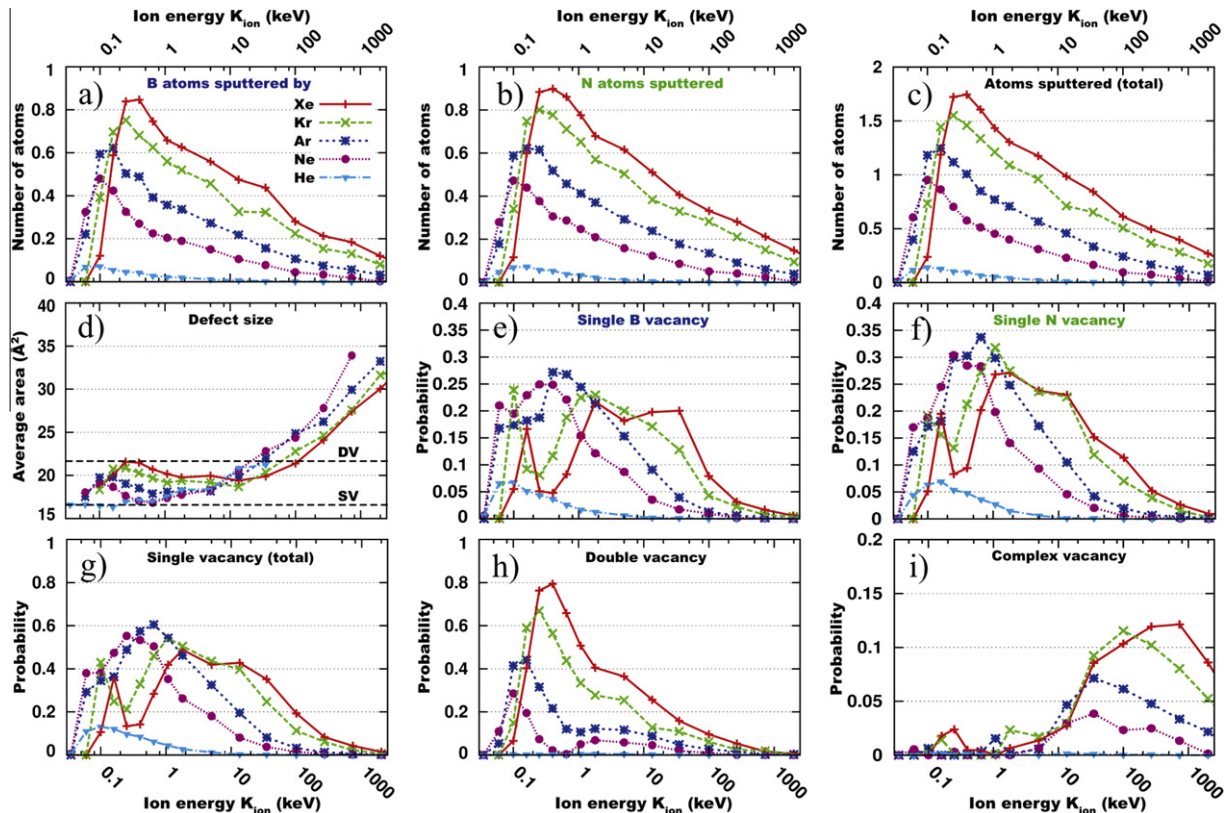


**Fig. 2.** Average numbers of sputtered atoms and probabilities for defect formations in a *h*-BN sheet after impacts of ions with a trajectory perpendicular to the sheet. (a) Average number of sputtered B atoms on a single ion impact for He, Ne, Ar, Kr and Xe ions as a function of energy. (b) Average number of sputtered N atoms. (c) Average number of any sputtered atoms. (d) Average size of a defect created under an ion impact. Probabilities of creating a single B vacancy (e), single N vacancy (f), any single vacancy (g), double vacancy (h), and complex vacancy (i) with a single ion impact.

displacement cross-section correspondingly decreases. This leads to diminishing probability of DV creation and again increasing probability of SVs.

At low to medium energies ( $< \sim 10$  keV, collision kinetics leads to recoil angles of the target atoms mostly out of the *h*-BN plane. Due to this, recoiled atoms leave the target system without creating further damage, as is evident from the abundance of SVs and DVs at these energies. However, as the ion velocity becomes higher, the time of interaction between a target atom and the fast ion becomes very short leading to the target atom being in practice immobile during the interaction. Thus, for an ion trajectory perpendicular to the sheet, the interaction is nearly symmetric in the out-of-plane direction, which leads to target atoms recoiling close to the in-plane direction. This results in complex vacancy (CV, one or more atoms missing, but not SV or DV) structures becoming the dominating defect type, Fig. 2(i). The increase in average defect size in terms of lost perfect hexagonal BN-rings is displayed in Fig. 2(d). However, we stress that collision cascades in 2D are rare events as compared to 3D collision cascades typically observed in bulk materials (note the y-axis scale in Fig. 2(i)).

When an atom is displaced from the *h*-BN structure, it is possible that it gets bonded to a neighboring atom and is not ejected from the system, but becomes an ad-atom or part of a reconstructed non-hexagonal structure. This results in formations of defect structures where no atoms are missing, categorized as amorphizations. At low ion energies the recoiled atoms have barely enough energy to escape the system and some of them get stuck to their nearby neighbors. At high ion energies the recoil angles are close the *h*-BN plane and the recoiled atoms interact with many other target atoms leading to increased probability of getting stuck as an ad-atom or as a part of a reconstructed structure. At all ener-

gies the probability for the appearance of an amorphous structure is less than 5%.

### 3.2. Oblique ion trajectories

When the angle of ion incidence is tilted away from the normal direction, the parameter space needed to be mapped grows considerably. In Fig. 3, probabilities for creation of the different defect types are presented for all the used ion types and energy ranges and selected out-of-plane angles  $\theta$ . Each data point is averaged over all in-plane angles  $\phi$  ( $\sim 1000$  runs per datapoint).

As evident from Fig. 3, changing the angle of incidence has a dramatic effect on defect production. As a general trend, the more the ion trajectory is tilted, the larger the created defects are, with complex vacancies being the overwhelmingly dominating defect type at  $\theta > 45^\circ$ .

Another feature is the shifting of the defect production maxima towards higher energies with increasing out-of-plane angle. The tilting of the ion direction counteracts the diminishing effect of increasing ion velocity to defect production probability as the projected atomic density of the target in the ion direction grows with increasing  $\theta$ .

At moderate angles and high energies the probability of creating a complex vacancy decreases. This can be attributed to the fact that at high ion velocities the recoiled atoms move in direction perpendicular to the direction of the velocity of the ion as was explained earlier. At normal angle of incidence this perpendicular direction is the in-plane direction of the target sheet, leading to complex defects through collision cascades. As the beam is tilted, the perpendicular direction becomes out-of-plane (barring two distinct

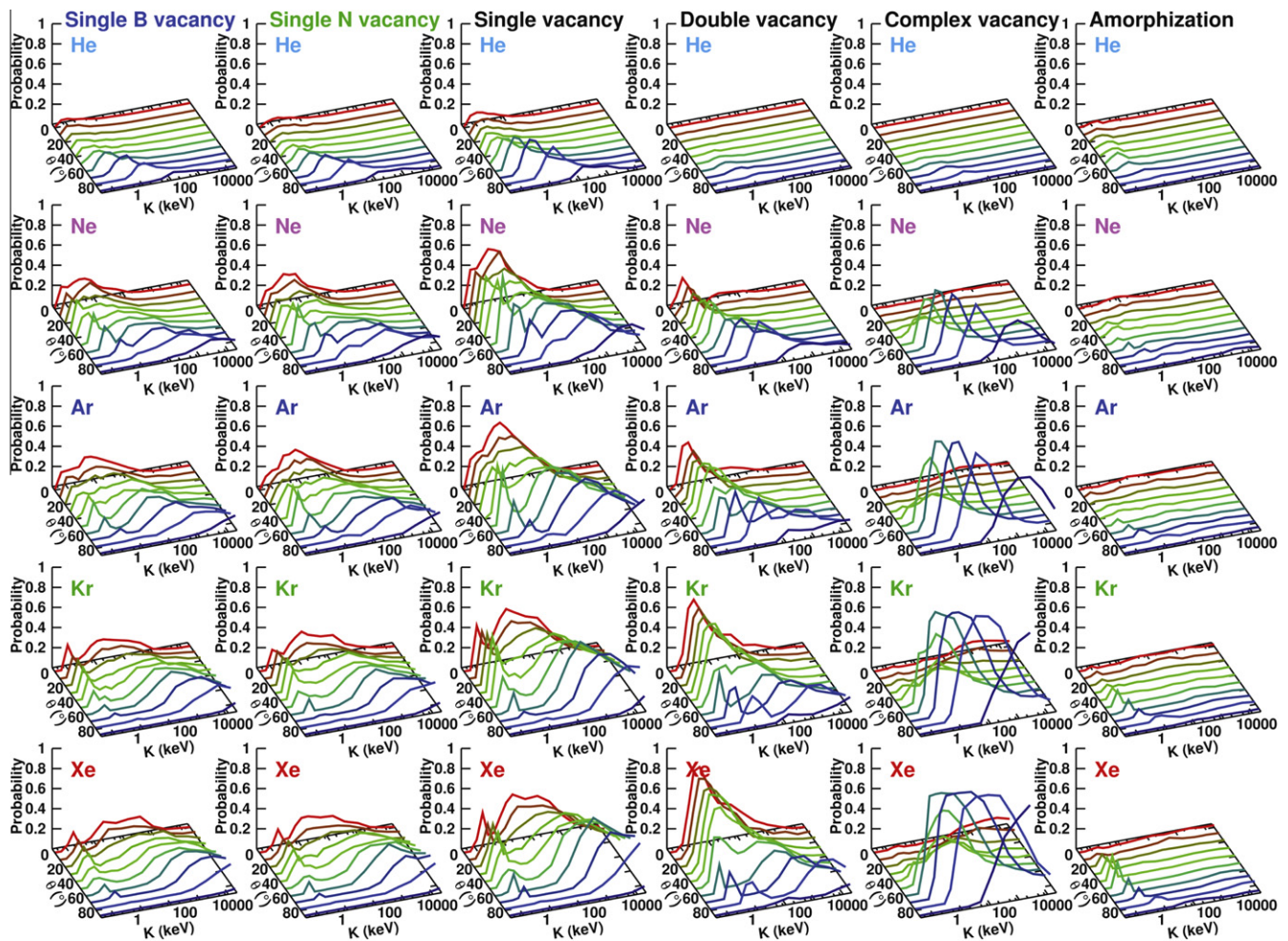


**Fig. 3.** Defect creation probabilities in *h*-BN monolayer under ion irradiation as a function of angle of incidence  $\theta$  and kinetic energy of the ion ( $K$ ), with defects categorized as single vacancies, double vacancies, complex vacancies and amorphous regions.

directions still in-plane). Hence most of the recoiled atoms escape the system without creating any further damage.

As evident from the presented data, varying the angle of ion incidence can have a high impact on the defect production probabilities in *h*-BN. This information can be of great use when designing new experiments on e.g. cutting of *h*-BN with a focused ion beam.

#### 4. Conclusions

The aim of this study was to gain a comprehensive picture of defect production in hexagonal boron nitride monolayer under energetic ion bombardment. As this information is not accessible through the standard methods (like TRIM) for estimating defect production under ion irradiation due to the low dimensionality of the target, molecular dynamics simulations of the impact events were conducted for a wide range of ion energies  $K \in [35 \text{ eV}, 10 \text{ MeV}]$ , species (He, Ne, Ar, Kr and Xe) and angles of incidence  $\theta \in [0, 88^\circ]$ . Approximately one million impact events were simulated in order to gain good statistics.

The produced defects were divided into four categories (single vacancies, double vacancies, complex vacancies and amorphizations). For ion direction perpendicular to the *h*-BN sheet, single vacancies (both B and N) were found to be the dominant defect types at a wide energy range (up to  $\sim 100 \text{ keV}$  for the heavier ions). The double vacancy probability maximum is located at the inter-

mediate energies ( $\sim 0.1\text{--}1.0 \text{ keV}$ ) reducing correspondingly the single vacancy probability. Complex vacancies dominate at high energies, with ultimately decreasing probabilities for ion energies in the MeV range. When the ion beam is tilted, the ratio between larger and smaller defects is altered. Amorphizations (modified morphology with no missing atoms) remain quite rare within the whole parameter space considered. This can be attributed to the binary structure of the target material and instability of bonds between atoms of the same species, which effectively inhibits reorganization of the structure without removal of atoms.

The presented data can be used for estimating the effects of ion irradiation in a hexagonal boron nitride monolayer under specific experimental conditions in terms of types of defects produced as well as number of sputtered target atoms and average sizes of defects produced. From another point of view, the fact that the probabilities of creating different types of defects reach their maxima at different ion energies implies that selectivity in produced defect types can be achieved through adjusting the ion irradiation parameters based on the presented data, which is an important result if engineering of *h*-BN nanosystems is to be conducted using ion irradiation.

Overall, we showed that unlike in a conventional three dimensional bulk target, the total number of displaced atoms from *h*-BN sheet is not a monotonous function of ion energy. The total number of defects does not necessarily increase with ion energy in such a two-dimensional system, contrary bulk solids. Moreover, deviations from the predictions of simple Kinchin–Pease-type model

[40] should be expected due to the reduced dimensionality of the system and lower probability for the development of collisional cascades. We also demonstrated that by tilting the sample, more control over the damage production during ion irradiation can be achieved in addition to simply selecting the ion energy. This is especially important when ion beam processing is carried out under conditions where ion energy cannot be freely selected, e.g., in a fixed-energy focused ion beam system.

## Acknowledgements

We thank the Finnish IT Center for Science for generous grants of computer time. This work was supported by the Academy of Finland through several projects and the Centre of Excellence programme.

## References

- [1] D. Pacilé, J.C. Meyer, Ç.Ö. Girit, A. Zettl, The two-dimensional phase of boron nitride: few-atomic-layer sheets and suspended membranes, *Appl. Phys. Lett.* 92 (2008) 133107.
- [2] N. Alem, R. Erni, C. Kisielowski, M.D. Rossell, W. Gannett, A. Zettl, Atomically thin hexagonal boron nitride probed by ultrahigh-resolution transmission electron microscopy, *Phys. Rev. B* 80 (2009) 155425.
- [3] A.K. Geim, K.S. Novoselov, The rise of graphene, *Nat. Mater.* 6 (2007) 183–191.
- [4] K. Watanabe, T. Taniguchi, H. Kanda, Direct-bandgap properties and evidence for ultraviolet lasing of hexagonal boron nitride single crystal, *Nat. Mater.* 3 (2004) 404–409.
- [5] V. Barone, J.E. Peralta, Magnetic boron nitride nanoribbons with tunable electronic properties, *Nano Lett.* 8 (8) (2008) 2210–2214.
- [6] B. Peng, M. Locascio, P. Zapol, S. Li, S.L. Mielke, G.C. Schatz, H.D. Espinosa, Measurements of near-ultimate strength for multiwalled carbon nanotubes and irradiation-induced crosslinking improvements, *Nat. Nanotech.* 3 (2008) 626–631.
- [7] J.A. Åström, A.V. Krasheninnikov, K. Nordlund, Carbon nanotube mats and fibers with irradiation-improved mechanical characteristics: a theoretical model, *Phys. Rev. Lett.* 93 (2004) 215503. 94, 0299(E) (2005).
- [8] A. Kis, G. Csányi, J.-P. Salvetat, T.-N. Lee, E. Coureau, A.J. Kulik, W. Benoit, J. Brugger, L. Förro, Reinforcement of single-walled carbon nanotube bundles by intertube bridging, *Nat. Mater.* 3 (2004) 153–157.
- [9] M.S. Raghuvver, A. Kumar, M.J. Frederick, G.P. Louie, P.G. Ganesan, G. Ramanath, Site-selective functionalization of carbon nanotubes, *Adv. Mater.* 18 (2006) 547–552.
- [10] Program TRIM (2008) by J.F. Ziegler and J.P. Biersack. Available from: <<http://www.srim.org>>.
- [11] O. Lehtinen, J. Kotakoski, A.V. Krasheninnikov, A. Tolvanen, K. Nordlund, J. Keinonen, Effects of ion bombardment on a two-dimensional target: atomistic simulations of graphene irradiation, *Phys. Rev. B* 81 (2010) 153401.
- [12] C. Jin, F. Lin, K. Suenaga, S. Iijima, Fabrication of a freestanding boron nitride single layer and its defect assignments, *Phys. Rev. Lett.* 102 (2009) 195505.
- [13] J.C. Meyer, A. Chuvilin, G. Algara-Siller, J. Biskupek, U. Kaiser, Selective sputtering and atomic resolution imaging of atomically thin boron nitride membranes, *Nano Lett.* 9 (2009) 2683–2689.
- [14] A. Celik-Aktas, J.F. Stubbins, J. Zuo, Electron beam machining of nanometer-sized tips from multiwalled boron nitride nanotubes, *J. Appl. Phys.* 102 (2007) 024310.
- [15] D. Golberg, Y. Bando, K. Kurashima, T. Sasaki, Boron-doped carbon fullerenes and nanotubes formed through electron irradiation-induced solid-state phase transformation, *Appl. Phys. Lett.* 72 (1998) 2108–2110.
- [16] J. Kotakoski, C.H. Jin, O. Lehtinen, K. Suenaga, A.V. Krasheninnikov, Electron knock-on damage in hexagonal boron nitride monolayers, *Phys. Rev. B* 82 (11) (2010) 113404.
- [17] A. Zobelli, A. Gloter, C.P. Ewels, C. Colliex, Shaping single walled nanotubes with an electron beam, *Phys. Rev. B* 77 (2008) 045410.
- [18] W. Orellana, H. Chacham, Stability of native defects in hexagonal and cubic boron nitride, *Phys. Rev. B* 63 (2001) 125205.
- [19] S. Azevedo, J.R. Kaschny, C.M.C. de Castilho, F. de Brito Mota, A theoretical investigation of defects in a boron nitride monolayer, *Nanotechnology* 18 (2007) 495707.
- [20] S. Okada, Atomic configurations and energetics of vacancies in hexagonal boron nitride: first-principles total-energy calculations, *Phys. Rev. B* 80 (2009) 161404.
- [21] L.-C. Yin, H.-M. Cheng, R. Saito, Triangle defect states of hexagonal boron nitride atomic layer: density functional theory calculations, *Phys. Rev. B* 81 (15) (2010) 153407.
- [22] A.V. Krasheninnikov, F. Banhart, Engineering of nanostructured carbon materials with electron or ion beams, *Nat. Mater.* 6 (2007) 723–733.
- [23] A.V. Krasheninnikov, K. Nordlund, Ion and electron irradiation-induced effects in nanostructured materials, *J. Appl. Phys.* 107 (2010) 071301.
- [24] K. Albe, Computersimulationen zu Struktur und Wachstum von Boronitrid, Ph.D. dissertation, der Technischen Universität Dresden, 1998.
- [25] K. Albe, W. Möller, Modelling of boron nitride: atomic scale simulations on thin film growth, *Comput. Mater. Sci.* 10 (1–4) (1998) 111–115.
- [26] H. Koga, Y. Nakamura, S. Watanabe, T. Yoshida, Molecular dynamics study of deposition mechanism of cubic boron nitride, *Sci. Technol. Adv. Mater.* 2 (2001) 349–356.
- [27] W.H. Moon, M.S. Son, J.H. Lee, H.J. Hwang, Molecular dynamics simulation of c60 encapsulated in boron nitride nanotubes, *Phys. Stat. Sol. (b)* 241 (2004) 1783–1788.
- [28] J.T. Yim, M.L. Falk, I.D. Boyd, Modeling low energy sputtering of hexagonal boron nitride by xenon ions, *J. Appl. Phys.* 104 (2008) 123507.
- [29] J.F. Ziegler, J.P. Biersack, U. Littmark, *The Stopping and Range of Ions in Matter*, Pergamon, New York, 1985.
- [30] J. Ullmann, J.E.E. Baglin, A.J. Kellock, Effects of MeV ion irradiation of thin cubic boron nitride films, *J. Appl. Phys.* 83 (1998) 2980–2987.
- [31] S. Mansouri, P. Marie, C. Dufour, G. Nouet, I. Monnet, H. Lebius, Swift heavy ions effects in iii–v nitrides, *Nucl. Instrum. Methods Phys. Res. Sect. B* 266 (2008) 2814–2818.
- [32] A.V. Krasheninnikov, Y. Miyamoto, D. Tománek, Role of electronic excitations in ion collisions with carbon nanostructures, *Phys. Rev. Lett.* 99 (2007) 016104.
- [33] H.J.C. Berendsen, J.P.M. Postma, W.F. van Gunsteren, A. DiNola, J.R. Haak, Molecular dynamics with coupling to external bath, *J. Chem. Phys.* 81 (8) (1984) 3684.
- [34] K. Nordlund, *PARCAS* computer code. The main principles of the molecular dynamics algorithms are presented in [41,42]. The adaptive time step and electronic stopping algorithms are the same as in [43] (2010).
- [35] A.V. Krasheninnikov, K. Nordlund, J. Keinonen, Production of defects in supported carbon nanotubes under ion irradiation, *Phys. Rev. B* 65 (2002) 165423.
- [36] A.V. Krasheninnikov, K. Nordlund, Multi-walled carbon nanotubes as apertures and conduits for energetic ions, *Phys. Rev. B* 71 (2005) 245408.
- [37] A. Tolvanen, J. Kotakoski, A.V. Krasheninnikov, K. Nordlund, Relative abundance of single and double vacancies in irradiated single-walled carbon nanotubes, *Appl. Phys. Lett.* 91 (2007) 173109.
- [38] J. Pomoell, A.V. Krasheninnikov, K. Nordlund, J. Keinonen, Stopping of energetic ions in carbon nanotubes, *Nucl. Instr. Meth. Phys. Res. B* 206 (2003) 18–21.
- [39] A.V. Krasheninnikov, Predicted scanning microscopy images of carbon nanotubes with atomic vacancies, *Solid State Comm.* 118 (2001) 361–365.
- [40] G.H. Kinchin, R.S. Pease, The displacement of atoms in solids by radiation, *Rep. Prog. Phys.* 18 (1955) 1.
- [41] K. Nordlund, M. Ghaly, R.S. Averback, M. Caturla, T. Diaz de la Rubia, J. Tarus, Defect production in collision cascades in elemental semiconductors and fcc metals, *Phys. Rev. B* 57 (13) (1998) 7556–7570.
- [42] M. Ghaly, K. Nordlund, R.S. Averback, Molecular dynamics investigations of surface damage produced by keV self-bombardment of solids, *Philos. Mag. A* 79 (4) (1999) 795.
- [43] K. Nordlund, Molecular dynamics simulation of ion ranges in the 1–100 keV energy range, *Comput. Mater. Sci.* 3 (1995) 448.